Journal of Crystallization Process and Technology, 2014, 4, 79-88
Published Online April 2014 in SciRes. http://www.scirp.org/journal/jcpt
http://dx.doi.org/10.4236/jcpt.2014.42011

Scientific Research

Low Pressure Chemical Vapor Deposition of Nb and F Co-Doped TiO_2 Layer

Satoshi Yamauchi*, Shouta Saiki, Kazuhiro Ishibashi, Akie Nakagawa, Sakura Hatakeyama

Department of Biomolecular Functional Engineering, Ibaraki University, Hitachi, Japan
Email: *ysatoshi@mx.ibaraki.ac.jp

Received 20 January 2014; revised 20 February 2014; accepted 27 February 2014

Copyright © 2014 by authors and Scientific Research Publishing Inc.
This work is licensed under the Creative Commons Attribution International License (CC BY).
http://creativecommons.org/licenses/by/4.0/

Open Access

Abstract

Nb and F co-doped anatase TiO_2 layers were deposited by low pressure chemical vapor deposition (LPCVD) at pressure of 3 mtorr using titanium-tetra-iso-propoxide (TTIP), O_2 and NbF_5 as precursor, oxidant and dopant respectively. Resistivity beyond 100 Ωcm for undoped layer was decreased with increasing supply of the dopant and dependent on the supply ratio of O_2 to TTIP and decreased to 0.2 Ωcm by the optimization. X-ray fluorescent spectroscopy showed Nb-content in the layer was decreased with the O_2-supply ratio. X-ray photo-spectroscopy indicated that F substituted O-site in TiO_2 by O_2-supply but carbon-contamination and F missing substitution in the O-site were significantly increased by excess O_2-supply. Further, it was suggested that the substituted F played an important role to reduce resistivity without significant contribution of O-vacancies. XRD spectra showed F missing substitution in the O-site degraded the crystallinity.

Keywords

LPCVD, Anatase-TiO_2, Nb and F Co-Doping, Low-Resistive TiO_2

1. Introduction

Nowadays, Indium-Tin-Oxide (ITO) is widely used for transparent conducting oxide (TCO) to fabricate flat panel displays, solar-cells and so on. However, the amount of Indium on earth is significantly low as shown by Clarke number. Therefore, the alternative TCO without Indium has been attractively studied, for example, Ga-doped ZnO (GZO), F-doped SnO_2 (FTO) etc. [1] [2]. TiO_2, which has been extensively investigated in view of photo-induced applications using the photo-catalytic reactions and the hydrophilicity [3] [4] in addition to dielectric applications using the high dielectric constant and optoelectronic applications by the high refractive index [5] [6], is also candidate for TCO because of the wide bandgap about 3.2 eV. It is however easily recognized

*Corresponding author.

How to cite this paper: Yamauchi, S., Saiki, S., Ishibashi, K., Nakagawa, A. and Hatakeyama, S. (2014) Low Pressure Chemical Vapor Deposition of Nb and F Co-Doped TiO_2 Layer. *Journal of Crystallization Process and Technology*, **4**, 79-88.
http://dx.doi.org/10.4236/jcpt.2014.42011

that the conductivity control of TiO_2 is more difficult than ZnO and Sn_2O since *d*-bands are included in the crystal. Therefore, precise control of the deposition condition using sufficient donor and the post-annealing required to control the conduction because not only the donor but also defect *d*-band due to Ti^{3+} generated by oxygen-deficiency contributes to the conduction. For the purpose, laser-ablation and reactive sputtering with the post-annealing have been recently studied by using Nb as a sufficient donor in anatase-TiO_2 [7] [8]. It is mentioned that oxygen-deficiency is required to enhance the electronic activation of the donor [9], which indicates the Ti^{3+} reduced from Ti^{4+} in TiO_2 contributes to the conduction, however, it is considered that the oxygen-vacancies cause the large lattice distortion and the insufficient stability. In contrast, it was reported that F substituted O-site in TiO_2 reduces Ti^{4+} to Ti^{3+} [10], in which the lattice distortion was significantly reduced comparing to oxygen-vacancy since the ion radius of F^- (0.136 nm) is close to O^{2-} (0.140 nm). It is therefore expected that F can play an important role in Nb-doped TiO_2 layer to increase the conductivity preventing the lattice distortion, but the study for Nb-F co-doping in TiO_2 has not been studied whereas F doping has been reported for the photo-activities [11] [12].

Conductivity controlled TiO_2 layers are also expected to use for such as chemical sensors, solar-cells, and the other electronic devices in solutions because of the high resistance against acid- and alkaline-electrolytes. For such device applications, chemical vapor deposition (CVD) is a useful process comparing to physical vapor deposition in the view of step-coverage on the three-dimensionally structured surfaces to enhance the sensitivity and the efficiency in addition to the micro-fabrication by reactive ion etching [13]. CVD of TiO_2 layer has been studied by using metalorganic precursor of titanium-tetra-iso-propoxide (TTIP: $Ti(O\text{-}i\text{-}C_3H_7)_4$ aiming at high-efficient photo-induced properties, but few study for the conductivity control has been reported.

In this paper, low-pressure CVD (LPCVD) by TTIP and O_2 mixed gas was applied for TiO_2 deposition to control conductivity by Nb-F co-dope using NbF_5 as the dopant with the studies by X-ray fluorescent spectroscopy, X-ray photo-spectroscopy and X-ray diffraction.

2. Experimental

2.1. Deposition of TiO_2 Layer

A bell-jar type reactor with the base pressure under 1×10^{-5} torr by a combination of diffusion pump (D.P.) and a rotary pump (R.P.) as shown in **Figure 1** was used for LPCVD of titanium-oxide. Titanium tetra-iso-propoxide (TTIP, $Ti(O\text{-}i\text{-}C_3H_7)_4$: 99.7%-purity) in liquid-phase was charged into a quartz cell and initially purified in vacuum at 50˚C for 3 hrs, then vaporized at 70˚C to introduce into the reactor through a stainless tube for TiO_2 deposition. The gas-phase TTIP was introduced without any carrier gas but pure oxygen gas (99.9999%-purity) was simultaneously introduced into the reactor through the other gas inlet. The supply ratio of O_2/TTIP was controlled by monitoring the reactor pressure using Shultz gage when the TTIP and the O_2 was individually in-

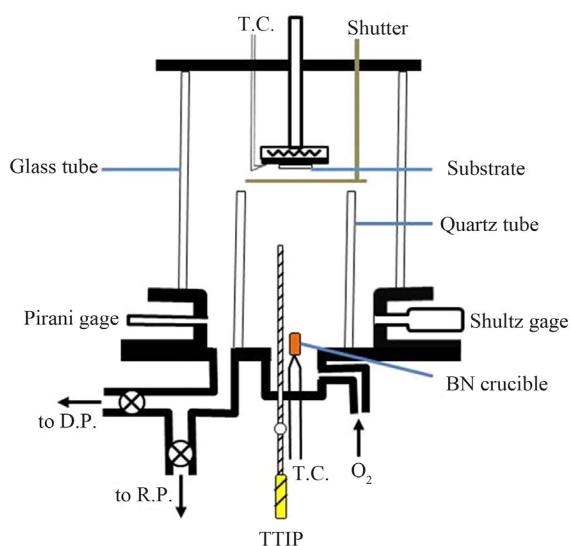

Figure 1. LPCVD apparatus for TiO_2 deposition.

troduced into the reactor. Niobium pentafluoride (NbF_5: 98%-purity) powder was charged in a crucible consists of boron-nitride (BN) and then thermally evaporated. 1 mm-thick quartz plate with optically flat surface was used as substrate, which was mounted on a substrate holder after chemical cleaning. Temperature of the substrate holder and the crucible were monitored by K-type thermo-couples (T.C.) and controlled by resistive heating and PID-systems.

2.2. Evaluation

Thickness of the layer was checked by a surface profiler (DEKTAK150). Resistivity was evaluated by Van Der Pauw (VDP) method. Densities and chemical states of impurities were analyzed by X-ray fluorescent spectroscopy (XRF: Shimazu XRF-1700) and X-ray photo-spectroscopy (XPS: Thermo VG Scientific,UK). Crystallographic behavior was examined by θ-2θ X-ray diffraction (RIGAKU: RAD-C) using CuK_α.

3. Results and Discussions

3.1. Dependence of Resistivity on the Deposition Condition

Figure 2 shows dependence of undoped-TiO_2 deposition rate on the deposition temperature in Arrhenius plot. The deposition rate was increased with the temperature by the activation energy of 138 kJ/mol then saturated above 360˚C. The activation energy using TTIP and O_2 was seemed to be larger than that in other reports demonstrated at relatively high pressure above 0.1 torr [14] [15] but similar to the value of 150 kJ/mol by CVD using TTIP in N_2-gas with the high flow rate [16]. It has been considered that dissociation of TTIP is enhanced by oxygen, however, the result indicated TTIP was thermally dissociated in such low pressure according to the previously reported schemes as below [17] [18],

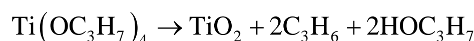

$$\mathrm{Ti(OC_3H_7)_4 \rightarrow TiO_2 + 2C_3H_6 + 2HOC_3H_7}$$

or

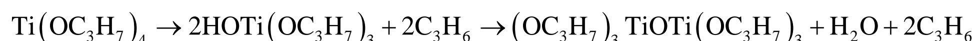

$$\mathrm{Ti(OC_3H_7)_4 \rightarrow 2HOTi(OC_3H_7)_3 + 2C_3H_6 \rightarrow (OC_3H_7)_3TiOTi(OC_3H_7)_3 + H_2O + 2C_3H_6}$$

In such feature, the deposition above 360˚C can be recognized to be limited by TTIP-supply. In this work, all samples for the study of Nb-F doping were deposited at 380˚C in the TTIP-supply limiting region for removal residual impurities such as carbon and/or hydrocarbons and to enhance crystallization into the anatase-phase.

Resistivity of the undoped-layer deposited at 380˚C was higher than 100 Ωcm because the resistivity was over the evaluation-limit in our VDP-system which was able to evaluate the resistivity below 100 Ωcm. On the other, the resistivity of Nb-F doped TiO_2 layer was significantly reduced with the crucible temperature for NbF_5 evaporation (T_{NbF5}) and dependent on O_2/(TTIP + O_2) gas supply ratio as shown in **Figure 3**. **Figure 3(a)** shows dependence of the resistivity (solid-circle and solid-line) and the deposition rate (open-circle and dot-line) on the T_{NbF5}, where the layers with the thickness about 200 nm were deposited by the O_2/(TTIP + O_2) supply ratio of 0.50. The resistivity was decreased with the T_{NbF5} below 70˚C and above 100˚C then saturated about 1 Ωcm at

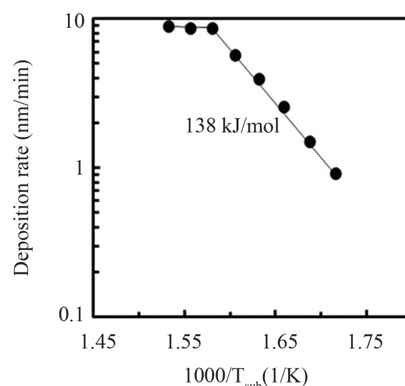

Figure 2. Arrhenius plot of TiO_2 deposition rate for the deposition temperature.

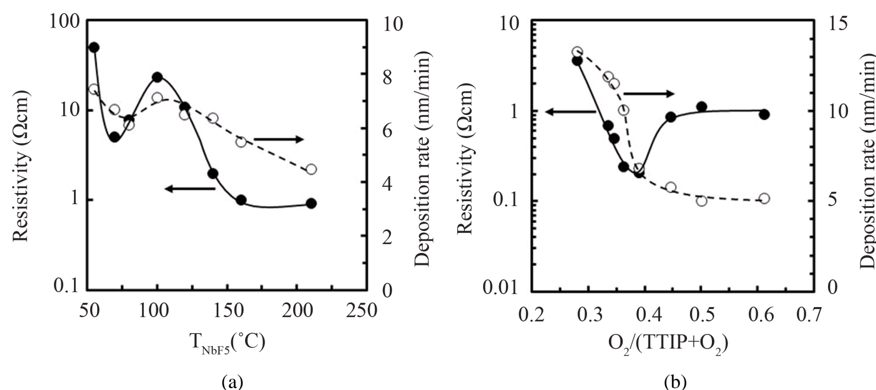

Figure 3. Resistivity (solid-circle and solid-line) and deposition rate (open-circle and dot-line) of Nb-F doped TiO_2 layer (a) deposited by gas supply ratio of $O_2/(TTIP + O_2) = 1.0$ at various Nb-F crucible temperature ($TNbF_5$), and (b) deposited by NbF_5 supply at the $TNbF_5 = 160˚C$ in various $O_2/(TTIP + O_2)$ supply ratio.

the T_{NbF5} above 160˚C, but increased in the range from 70 to 100˚C. The increase of resistivity with the T_{NbF5} was due to melt of NbF_5 at the temperature above 70˚C, that is, the NbF_5 was sublimated below 70˚C and evaporated above 100˚C after melting. It is noted that the carrier density and Hall mobility could not be determined by the VDP-system because of trap-induced conductions such as hopping, but conventional check by Zeebeck effect showed n-type conductivity for the doped layers. In addition to the decrease of resistivity, the deposition rate was decreased with NbF_5-supply as shown by open circles in **Figure 3(a)**, which indicated the dopant influenced dissociation of TTIP. The feature for deposition rate influenced by NbF_5 was also dependent on O_2-supply ratio as shown by open-circles in **Figure 3(b)**, where the NbF_5 was evaporated at 160˚C. It is noted that total gas pressure of TTIP + O_2 for the various gas ratio was kept at 3 mtorr, therefore, the deposition rate of undoped layer was linearly decreased with the O_2-partial pressure according to decrease of TTIP-supply rate. However, the deposition rate of Nb-F doped layer was non-linearly decreased with the O_2-supply ratio, especially, above 0.35. For example, deposition rate of the doped layer deposited by the gas-supply ratio of 0.50 was 5 nm/min whereas the rate was 9 nm/min for undoped layer as shown in **Figure 1**. Since TTIP was thermally dissociated without oxidation, the obvious decrease of deposition rate for the doped layer could be recognized to be caused by reactive species dissociated from NbF_5 by the oxidation. On the other, the resistivity of the doped layer with the thickness about 200 nm was decreased with the O_2-supply ratio and as low as 0.2 Ωcm by the O_2-supply ratio of 0.38, but increased with the O_2-supply ratio above 0.40 and then saturated about 1 Ωcm. As a result, the O_2-supply for the deposition rate and the resistivity could be considered in three-regions such as Region I: poor O_2-supply (O_2 supply ratio under 0.38,) Region II; sufficient O_2-supply (O_2 supply ratio about 0.38), Region III; excess O_2-supply (O_2 supply ratio beyond 0.38).

3.2. XRF and XPS Evaluations

Figure 4 shows XRF spectra of Nb-F doped layers deposited by the $O_2/(TTIP + O_2)$ supply ratio of 0.27 in Region I (green-line), 0.38 in Region II (black-line) and 0.61 in Region III (red-line) respectively where NbF_5 was evaporated at the T_{NbF5} of 160˚C. Background in the spectra was numerically removed by poly-nominal function and then the spectra were normalized by the Ti-K_α intensity. The intensity due to Nb-K_α was decreased with the O_2-supply ratio, which resultantly indicated Nb-content was decreased with the gas supply ratio as shown in the inset. Because the deposition rate was decreased with the gas-supply ratio for same supply rate of NbF_5 (**Figure 3(b)**), the variation of Nb-content could not be simply discussed on the dopant-supply rate for the deposition rate. It is expected that $NbOF_x$ and F were formed from NbF_5 by the oxidation, and the density on the deposition surface were increased with O_2-supply rate. While Nb-content in the layer should be increased with the density of $NbOF_x$ on the surface because of the sticking probability higher than NbF_5, the experimental result in **Figure 4** showed reversal dependence. Therefore, it is speculated that F dissociated from NbF_5 was an important species to clarify the doping, however, the content in the layers could not be evaluated by XRF because X-ray emission rate of the element was significantly low in addition to the low concentration in the layer. In contrast, the element could be studied on the chemical states by XPS. **Figure 5** shows high resolution (a) C1s and (b) F1s XPS

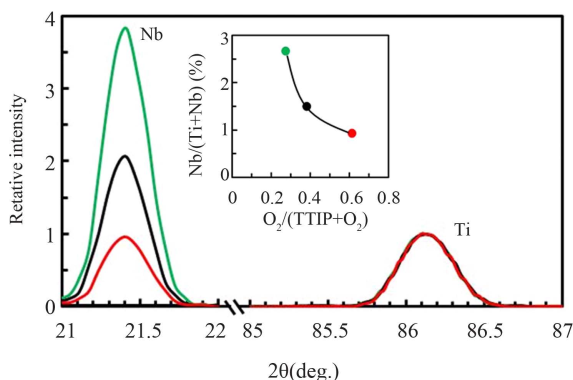

Figure 4. XRF spectra for Nb-K_a (Nb) and Ti-K_a (Ti) of Nb-F doped TiO_2 layers deposited by $O_2/(TTIP + O_2)$ supply ratio of 0.27 (green-line), 0.38 (black-line) and 0.61 (red-line), where the intensity was normalized by the intensity of Ti-K_a. The inset shows the evaluated Nb-content.

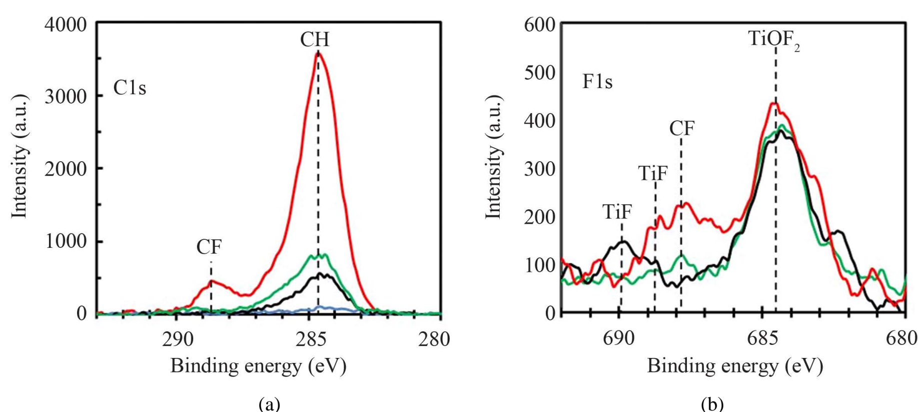

Figure 5. (a) C1s and (b) F1s XPS spectra of Nb-F doped TiO_2 layers deposited by various $O_2/(TTIP + O_2)$ supply ratio of 0.28 (green-line), 0.38 (black-line) and 0.61 (red-line). The dot line in the (a) shows the spectrum of undoped TiO_2 layer deposited by the supply ratio of 0.50.

spectra of Nb-F doped TiO_2 layers deposited by the $O_2/(TTIP + O_2)$ supply ratio of 0.27 (green-line), 0.38 (black-line) and 0.61 (red-line) respectively, with the C1s spectrum of undoped layer by the O_2-supply ratio of 0.50 (blue-line). It is noted that the spectrum originated from Nb was under detectable limit. Extremely weak C1s spectrum peak at 284.3 eV was appeared on the undoped layer, which indicated TTIP was successfully dissociated to TiO_2. On the other, significantly increased spectra were observed in the doped layers depending on the O_2-supply ratio, where the peak energy was shifted to 284.7 eV. Although the peak at 284.3 could be assigned to physisorbed carbons, the shift of peak-energy and the obvious increase of intensity indicated that the origin was not only adventitious carbons but also carbon-compounds included in the layers. Recently, Karlsson *et al*. studied TTIP-dissociation in ultra-high vacuum by XPS and showed C1s spectra peak at 285 eV is attributed to adsorbed methyl-group originated from TTIP [19]. Additionally, in the case of the layer deposited by the excess O_2-supply rate in Region III, spectrum in higher energy side was appeared at 288.5 eV. A lot of study for fluorinated hydro-carbons have been achieved by XPS and indicated that the spectra above 288 eV is originated from fluorinated carbon [20] [21]. It is consequently considered that alcohol group in TTIP was fluorinated in the condition of Region III, which was resulted in decrease of the deposition rate as shown in **Figure 3** and increase of the residual methyl-group indicated by obvious increase of the spectrum peak at 284.7 eV. The fluorination was also observed in F1s spectra as shown in **Figure 5(b)**. In the spectra, the most intense spectra peak at 684.5 could be attributed to adsorbed F ion or $TiOF_2$-F [22]. The spectrum peak at 688 assigned to C-F [23] was intense for the layer deposited by the excess O_2-supply rate (red-line), in which the intensity of C1s spectrum due to fluorinated carbon peak at 288.5 eV was also appeared. The other spectra peak at 689 eV and

690 eV could be assigned to F substituted in O-site of TiO_2 [24] [25]. The results indicated F could be doped in the O-site by O_2-supply in Region II and III. It is interesting that the result suggested the electronic activation efficiency of Nb in the layer was increased by the substituted F because resistivity of the layer deposited by the gas-supply ratio of 0.27 in Region I was significantly high comparing to the layer by the gas-supply ratio of 0.38 in Region II whereas the Nb-content was decreased with the gas-supply ratio.

The role of oxygen has been in progress by first-principles molecular-orbital calculations, but it can be expected as follows.

<Scheme 1: Without oxygen-contribution>

NbF_5 is adsorbed on the deposition surface (probably to titanium) where H_2O formed during Ti-O-Ti bridging from Ti-OH---OH-Ti is simultaneously supplied to the NbF_5, then the NbF_5 is oxidized and HF is desorbed from the surface as the below scheme.

$$\mathrm{NbF_5} + n\mathrm{H_2O} \rightarrow \mathrm{NbO}_n\mathrm{F}_{5-2n} + 2n\mathrm{HF}\uparrow$$

In this scheme, F-content in the layer is decreased with H_2O-density on the surface.

<Scheme 2: With oxygen contribution>

NbF_5 adsorbed on the deposition surface is dissociated by oxygen as follow scheme, and then the dissociated F with the high reactivity adsorbs to titanium on the surface with high sticking probability or fluorinates the TTIP.

$$\mathrm{NbF_5} + m\mathrm{O_2} \rightarrow \mathrm{NbO}_{2m}\mathrm{F}_{5-2m} + 2m\mathrm{F}\uparrow$$

The adsorbed F decreases the sticking probability of the next coming NbF_5 and TTIP, which resultantly decreases Nb-content in the layer and the deposition rate. Further, the fluorination disturbs thermal dissociation of TTIP, which is resulted in decreased of the deposition rate and increase of residual carbons in the layer. Of course, the dissociation of NbF_5 by H_2O as shown in the Scheme 1 is also including during the deposition but the oxygen-contribution becomes dominant by the high O_2-supply ratio according to the increased O_2-partial pressure comparing to H_2O on the surface.

Figure 6 shows the content ratio of F/Ti (solid-circle) and F/Nb (open-circle) in the layers for various $O_2/(TTIP + O_2)$ supply ratio, where the ratio of F/Nb was estimated by the F/Ti ratio obtained by XPS and the Nb/Ti ratio evaluated by XRF. The F/Ti ratio was significantly increased by the high O_2-supply ratio in Region III. On the other, F was excessively contained in the layer than Nb (F/Nb > 1.0) and the F/Nb ratio was uniquely increased with the O_2-supply ratio. These results indicated that F was easily introduced into the layer by supporting of oxygen whereas the Nb-content was decreased with the O_2-supply, which was consistent with the result expected by the Sequence 1 and the Sequence 2.

Oxygen chemical state in the layer was also influenced by the $O_2/(TTIP + O_2)$ supply ratio. **Figure 7** shows O1s XPS spectra of Nb-F doped layers deposited by the gas-supply ratio of 0.27 (green-line), 0.38 (black-line) and 0.61 (red-line) with the spectrum of undoped layer by the gas ratio of 0.50 (blue-line), where the deconvo-

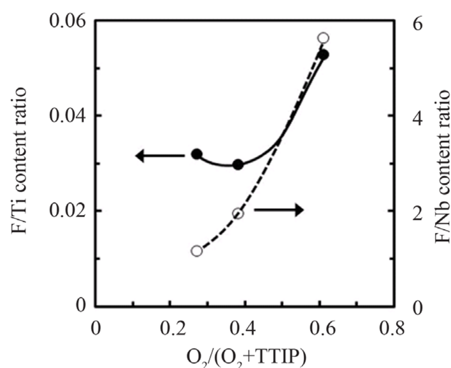

Figure 6. F/Ti content ratio evaluated by XPS (solid-circle and left-axis) and estimated F/Nb content ratio from XPS and XRF data (open-circle and right-axis) for $O_2/(TTIP + O_2)$ supply ratio.

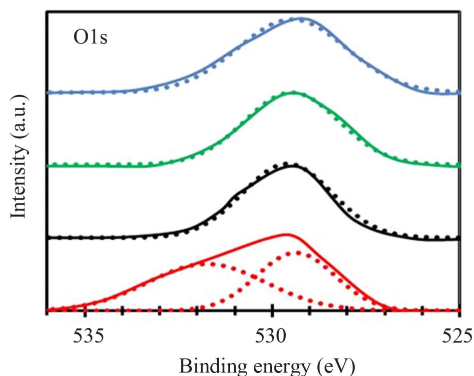

Figure 7. O1s XPS spectra of Nb-F doped TiO_2 layers deposited by various $O_2/(TTIP + O_2)$ supply ratio of 0.28 (green-line), 0.38 (black-line) and 0.61 (red-line) with the spectrum of undoped layer (blue-line) deposited by the gas supply ratio of 0.50. The dot lines show the deconvoluted spectra performed by Gaussian function.

luted spectra using Gaussian-function were also shown by dot-lines. Single spectrum peak at 529.5 eV were observed for the undoped and the doped layers deposited by the gas ratio of 0.27 and 0.38, but the other spectrum peak at 531.9 eV was also included for the doped layer by high O_2-supply ratio of 0.61. Previously, the double spectra was discussed for ITO layers, in which the spectrum at low high energy is concluded to be originated from oxygen neighboring cations coordinated six oxygens but the spectrum is shifted toward higher energy-side by contribution of oxygen-vacancies [26]. It is simply considered that oxygen-deficiency is reduced by increase of O_2-supply ratio. However, the results shown in **Figure 7** indicated the oxygen-vacancies were significantly increased by high O_2-supply rate in Region III, which could be concluded that excess fluorine dissociated from NbF_5 caused the oxygen-vacancies. Commonly, annealing to reduce resistivity of Nb-doped TiO_2 layers has been processed in vacuum or reduction environment since oxygen-vacancies play an important role to reduce resistivity [27] [28]. In contrast, resistivity of the Nb-F doped layer was decreased with the O_2-supply rate in Region I and Region II as shown in **Figure 3(b)**, but the density of oxygen-vacancies were not increased. The result apparently indicated fluorine substituted to oxygen in TiO_2 was important to reduce the resistivity of the Nb-F doped layer without the contribution of oxygen-vacancies. Further, the resistivity was increased in Region III whereas the density of oxygen-vacancy was significantly increased.

3.3. Crystallographic Property

Figure 8 shows θ-2θ XRD spectra of Nb-F doped TiO_2 layers with the spectrum of undoped layer (blue-line) deposited by $O_2/(TTIP + O_2)$ supply ratio of 0.50, where the doped layers were deposited by the gas supply ratio of 0.27 (green-line), 0.38 (black-line) and 0.61 (red-line) with the dopant evaporation at 160˚C. The spectra revealed the layers were poly-crystallized into the anatase-phase without the other phase such as rutile, brookite and the other compound as $TiOF_2$. The inset shows the spectra around anatase-TiO_2 (101) diffraction peak. The diffraction peak at $2\theta = 25.32^{\circ}$ for the undoped layer was slightly shifted toward larger angle comparing to $\theta = 25.28^{\circ}$ comparing to that of the bulk [29], which indicated tensile stress was induced in the layer due to difference of thermal expansion coefficient between the layer and the quartz substrate. On the other, the peak angle was 25.29° for the layers deposited by the O_2-supply ratio of 0.27 and 0.38, and 25.25° for the layer deposited by the gas-supply ratio of 0.61. Previously, it was reported that the peak angle is decreased (the *d*-spacing is increased) with Nb-content in Nb-doped TiO_2 layer fabricated by sputtering deposition and the post-annealing [27]. In this work, it is believed the mismatch for the ion radius between Ti^{4+} (0.061 nm) and Nb^{5+} (0.064 nm) in the cation-site was compensated by fluorine ion radius (F^-: 0.136 nm) smaller than that of oxygen ion (O^{2-}: 0.140 nm) in anion-site. However, the peak angle for the doped layers was shifted toward low angle-side comparing to that of the undoped-layer. Since Nb-content in the layers was decreased with the O_2-supply ratio and F-content was significantly increased by the gas-supply ratio of 0.61 as shown in **Figure 4** and **Figure 6**, the

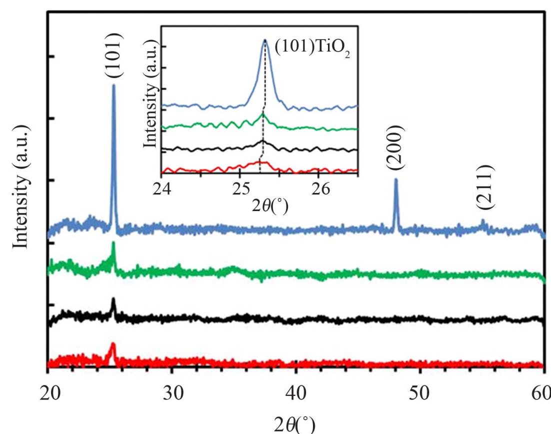

Figure 8. XRD spectra of undoped (blue-line) deposited by O_2/(TTIP + O_2) supply ratio of 0.50 and Nb-F doped TiO_2 layers deposited by O_2/(TTIP + O_2) supply ratio of 0.27 (green-line), 0.38 (black-line) and 0.61 (red-line), where NbF_5 was supplied at the crucible temperature of 160˚C.

peak angle should be shifted toward high angle-side (decrease of the *d*-spacing) comparing to that of the layers deposited in Region I and Region II. It is therefore difficult to recognize that the shift was due to the substituted Nb and F and expected to be caused by the fluorine missing the substitution in the oxygen site without crystallization into $TiOF_2$. As a result, it could be mentioned that removal the insufficient fluorine is required to improve crystallinity for further reduction of the resistivity.

4. Conclusion

Nb and F were simultaneously doped in anatase-TiO_2 by using NbF_5 on low pressure chemical vapor deposition using TTIP and O_2. Nb and F-content in the layer were dependent on the O_2-supply ratio, in which the Nb-content was decreased with increasing the gas supply ratio but F was increased in the high gas-supply ratio. XPS studies indicated F substitutes O-site in TiO_2 by the O_2-supply but carbon contamination is also increased by the excess O_2-supply. It was suggested by comparison between the resistivity and the XPS results that F in the O-site plays an important role to reduce the resistivity without oxygen-vacancies. XRD spectra speculated F missing substitution in the O-site degrades the crystallinity.

References

[1] Assunção, V., Fortunato, E., Marques, A., Águas, H., Ferreira, I., Costa, M.E.V. and Martins, R. (2003) Influence of the Deposition Pressure on the Properties of Transparent and Conductive ZnO:Ga Thin-Film Produced by r.f. Sputtering at Room Temperature. *Thin Solid Films*, **427**, 401-405. http://dx.doi.org/10.1016/S0040-6090(02)01184-7

[2] Lewis, B.G. and Paine, D.C. (2000) Applications and Processing of Transparent Conducting Oxides. *MRS Bulletin*, **25**, 22-27. http://dx.doi.org/10.1557/mrs2000.147

[3] Wang, R., Hashimoto, K. and Fujishima, A. (1997) Light-Induced Amphiphilic Surfaces. *Nature*, **388**, 431-432. http://dx.doi.org/10.1038/41233

[4] Mills, A., Lepre, A., Elliott, N., Bhopal, A., Parkin, I.P. and Neill, S.A. (2003) Characterisation of the Photocatalyst Pilkington Activ^{TM}: A Reference Film Photocatalyst? *Journal of Photochemistry and Photobiology A*: *Chemistry*, **160**, 213-224. http://dx.doi.org/10.1016/S1010-6030(03)00205-3

[5] Campbell, S.A., Kim, H.S., Gilmer, D.C., He, B., Ma, T. and Gladfelter, W.L. (1999) Titanium Dioxide (TiO_2)-Based Gate Insulators. *IBM Journal of Research and Development*, **43**, 383-392. http://dx.doi.org/10.1147/rd.433.0383

[6] Martinet, C., Paillard, V., Gagnaire, A. and Joseph, J. (1997) Deposition of SiO_2 and TiO_2 Thin Films by Plasma Enhanced Chemical Vapor Deposition for Antireflection Coating. *Journal of Non-Crystalline Solids*, **216**, 77-82.

http://dx.doi.org/10.1016/S0022-3093(97)00175-0

[7] Hitosugi, T., Ueda, A., Furubayashi, Y., Hirose, Y., Konuma, S., Shimada, T. and Hasegawa, T. (2006) Fabrication of TiO_2-Based Transparent Conducting Oxide Films on Glass by Pulsed Laser Deposition. *Japanese Journal of Applied Physics*, **46**, L86-L88. http://dx.doi.org/10.1143/JJAP.46.L86

[8] Gillispie, M.A., van Hest, M.F.A.M., Dabney, M.S., Perkins, J.D. and Ginley, D.S. (2007) rf Magnetron Sputter Deposition of Transparent Conducting Nb-doped TiO_2 Films on $SrTiO_3$. *Journal of Applied Physics*, **101**, 033125-1-4. http://dx.doi.org/10.1063/1.2434005

[9] Hoang, N.L., Yamada, N., Hitosugi, T., Kasai, J., Nakao, S., Shimada, T. and Hasegawa, T. (2008) Low-temperature Fabrication of Transparent Conducting Anatase Nb-doped TiO_2 Films by Sputtering. *Applied Physics Express*, **1**, 115001-115003. http://dx.doi.org/143/APEX.1.115001

[10] Di Valentin, C., Pacchioni, G. and Selloni, A. (2009) Reduced and n-Type Doped TiO_2: Nature of Ti^{3+} Species. *Journal of Physical Chemistry C*, **113**, 20543–20552. http://dx.doi.org/10.1021/jp9061797

[11] Li, D., Haneda, H., Hishita, S., Ohashia, N. and Labhsetwar, N.K. (2005) Fluorine-doped TiO_2 Powders Prepared by Spray Pyrolysis and Their Improved Photocatalytic Activity for Decomposition of Gas-phase Acetaldehyde. *Journal of Fluorine Chemistry*, **126**, 69-77. http://dx.doi.org/10.1016/j.jfluchem.2004.10.044

[12] Di Valentin, C., Finazzi, E., Pacchioni, G., Selloni, A., Livraghi, S., Czoska, A.M., Paganini, M.C. and Giamello, E. (2008) Density Functional Theory and Electron Paramagnetic Resonance Study on the Effect of N-F Codoping of TiO_2. *Chemistry of Materials*, **20**, 3706-3714. http://dx.doi.org/10.1021/cm703636s

[13] Norasetthekul, S., Park, P.Y., Baik, K.H., Lee, K.P., Shin, J.H., Jeong, B.S., Shishodia, V., Lambers, E.S., Norton, D.P. and Pearton, S.J. (2001) Dry Etch Chemistries for TiO_2 Thin Films. *Applied Surface Science*, **185**, 27-33. http://dx.doi.org/10.1016/S0169-4332(01)00562-1

[14] Yang, W. and Wolden, C.A. (2006) Plasma-Enhanced Chemical Vapor Deposition of TiO_2 Thin Films for Dielectric Applications. *Thin Solid Films*, **515**, 1708-1713. http://dx.doi.org/10.1016/j.tsf.2006.06.010

[15] Ahn, K.H., Park, Y.B. and Park, D.W. (2003) Kinetic and Mechanistic Study on the Chemical Vapor Deposition of Titanium Dioxide Thin Films by *In Situ* FT-IR using TTIP. *Surface Coating and Technology*, **171**, 198-204. http://dx.doi.org/10.1016/S0257-8972(03)00271-8

[16] Yokozawa, M., Iwasa, H. and Teramoto, I. (1968) Vapor Deposition of TiO_2. *Japanese Journal of Applied Physics*, **7**, 96-97. http://dx.doi.org/10.1143/JJAP.7.96

[17] Fictorie, C.P., Evans, J.F. and Gladfelter, W.L. (1994) Kinetic and Mechanistic Study of the Chemical Vapor Deposition of Titanium Dioxide Thin Films using Tetrakis-(Isopropoxo)-Titanium (IV). *Journal of Vacuum Science & Technology A*, **12**, 1108-1113. http://dx.doi.org/10.1116/1.579173

[18] Chen, S., Mason, M.G., Gysling, H.J., Paz-Pujalt, G.R., Blanton, T.N., Castro, T., Chen, K.M., Fictorie, C.P., Gladfelter, W.L., Franciosi, A., Cohen, P.I. and Evans, J.F. (1993) Ultrahigh Vacuum Metalorganic Chemical Vapor Deposition Growth and *In Situ* Characterization of Epitaxial TiO_2 Films. *Journal of Vacuum Science & Technology A*, **11**, 2419-2429. http://dx.doi.org/10.1116/1.578587

[19] Karlsson, P.G., Richter, J.H., Andersson, M.P., Johansson, M.K.-J., Blomquist, J., Uvdal, P. and Sandell, A. (2011) TiO_2 Chemical Vapor Deposition on Si(111) in Ultrahigh Vacuum: Transition from Interfacial Phase to Crystalline Phase in the Reaction Limited Regime. *Surface Science*, **605**, 1147-1156. http://dx.doi.org/10.1016/j.susc.2011.03.001

[20] Schmidt, S., Goyenola, C., Gueorguiev, G.K., Jensen, J., Greczynski, G., Ivanov, I.G., Czigány, Zs. and Hultman, L. (2013) Reactive High Power Impulse Magnetron Sputtering of CF_x Thin Films in Mixed Ar/CF_4 and Ar/C_4F_8 Discharges. *Thin Solid Films*, **542**, 21-30. http://dx.doi.org/10.1016/j.tsf.2013.05.165

[21] Crassous, I., Groult, H., Lantelme, F., Devilliers, D., Tressaud, A., Labrugère, C., Dubois, M., Belhomme, C., Colisson, A. and Morel, B. (2009) Study of the Fluorination of Carbon Anode in Molten KF-2HF by XPS and NMR Investigations. *Journal of Fluorine Chemistry*, **130**, 1080-1085. http://dx.doi.org/10.1016/j.jfluchem.2009.07.022

[22] Liu, G., Sun, C., Cheng, L., Jin, Y., Lu, H., Wang, L., Smith, S.C., Lu, G.Q. and Cheng, H.-M. (2009) Efficient Promotion of Anatase TiO_2 Photocatalysis via Bifunctional Surface-Terminating Ti-O-B-N Structures. *The Journal of Physical Chemistry C*, **113**, 12317-12324. http://dx.doi.org/10.1021/jp900511u

[23] Chiang, C.Y., Reddy, M.J. and Chu, P.P. (2004) Nano-Tube TiO_2 Composite PVdF/$LiPF_6$ Solid Membranes. *Solid State Ionics*, **175**, 631-635. http://dx.doi.org/10.1016/j.ssi.2003.12.039

[24] Yang, G., Wang, T., Yang, B., Yan, Z., Ding, S. and Xiao, T. (2013) Enhanced Visible-Light Activity of F-N Co-Doped TiO_2 Nanocrystals via Nonmetal Impurity, Ti^{3+} Ions and Oxygen Vacancies. *Applied Surface Science*, **287**, 135-142. http://dx.doi.org/10.1016/j.apsusc.2013.09.094

[25] Li, Y., Jiang, Y., Peng, S. and Jiang, F. (2010) Nitrogen-Doped TiO_2 Modified with NH_4F for Efficient Photocatalytic Degradation of Formaldehyde under Blue Light-Emitting Diodes. *Journal of Hazardous Materials*, **182**, 90-96.

http://dx.doi.org/10.1016/j.jhazmat.2010.06.002

[26] Fan, J.C.C. and Goodenough, J.B. (1977) X-Ray Photoemission Spectroscopy Studies of Sn-Doped Indium-Oxide Films. *Journal of Applied Physics*, **4B**, 3524-3531. http://dx.doi.org/10.1063/1.324149

[27] Sato, Y., Akizuki, H., Kamiyama, T. and Shigesato, Y. (2008) Transparent Conductive Nb-Doped TiO_2 Films Deposited by Direct-Current Magnetron Sputtering using a TiO_{2-x} Target. *Thin Solid Films*, **516**, 5758-5762. http://dx.doi.org/10.1016/j.tsf.2007.10.047

[28] Yu, C.-F., Sun, S.-J. and Chen, J.-M. (2014) Magnetic and Electrical Properties of TiO_2:Nb Thin Films. *Applied Surface Science*, **292**, 773-776. http://dx.doi.org/10.1016/j.apsusc.2013.12.047

[29] Weisssmann, S., *et al.* (1978) Selected Powder Diffraction Data for Metals and Alloys. JCPDS, Card No. 21-1272, 263.